Rotationally induced dissipation in superfluid helium

Michele Bonaldi and Stefano Vitale
Dipartimento di Fisica, Università degli Studi di Trento, I-38050 Povo, Trento, Italy
and Gruppo di Trento, Istituto Nazionale di Fisica Nucleare, I-38050 Povo, Trento, Italy

Massimo Cerdonio*
Laboratori Nazionali di Legnaro, Istituto Nazionale di Fisica Nucleare, I-35020 Legnaro, Padova, Italy
(Received 7 March 1990; revised manuscript received 27 June 1990)

In an attempt to make a superfluid ^{4}He analog of the radio-frequency superconducting quantum interference device (SQUID) that could be used as a gyroscope, we measured the critical velocity of the ac superflow through an orifice 5 μm in radius. The orifice was supported by a septum placed inside a hollow torus filled with liquid helium. The superflow through the orifice was induced by rotating the whole torus. The torus was the inertial member of a high-quality-factor torsion pendulum forced to oscillate at its resonance frequency. The occurrence of dissipation was detected by analyzing the oscillator motion. The principle on which this device works is analyzed, and results are reported of experiments in which quite reproducible critical oscillation amplitudes—well accounted for by intrinsic vortex formation—were obtained. Depending on the value of the forcing torque, the critical behavior manifested itself either as the occurrence of sudden collapses of the oscillation amplitude or as a steady excess dissipation. The energy involved in the process was estimated. Temperature dependencies of the critical amplitude up to 2.115±0.003 K were measured. The results were found to be in agreement both with the ac data obtained with the Helmholtz-resonator technique and with the data obtained with dc flow measurements.

I. INTRODUCTION

The superfluid component of liquid ^{4}He behaves as an irrotational ideal fluid flowing without friction up to a critical velocity v_c, at which dissipation sets in.[1]

The onset of this dissipation in the flow of superfluid helium through a small orifice has been investigated by many authors. Most of them studied the effects produced by temperature and by remnant vorticity in the helium bath, thus demonstrating the existence of two kinds of critical velocity. The first one, known as extrinsic velocity, typically almost independent of temperature, is typically a few 10^{-2} m/sec and cannot be made reproducible.[2] The other one, known as intrinsic velocity, is typically dependent on temperature, is reproducible within 1% and seems not to be correlated with the hole size,[3–9] its typical value is about $\sim$3 m/sec at 1 K.

The dissipation related to the intrinsic critical velocity was first observed as it led to the saturation of the gravitationally induced dc flow between two vessels connected by a micrometric orifice.[3,4] More recently it has also been observed to lead to the saturation of the oscillation amplitude of a Helmholtz resonator, where the flow through a hole is induced by an externally driven moving diaphragm.[5–9]

Both dc (Refs. 3 and 4) and ac (Refs. 8 and 9) flow measurements contribute to building up the following empirical pattern of behavior for the intrinsic critical velocity: v_c is well fitted by a linearly decreasing function of temperature from 5 mK up to $\sim$1.9 K, where its value is of the order of 1 m/sec. Above $\sim$1.9 K, where, however, only dc data are available, v_c is a steep decreasing function of temperature and it vanishes at T_λ.

In the commonly accepted interpretation, the dissipation in the superfluid flow is due to the creation and motion of superfluid quantized vortices in the liquid.[10] Consequently, the two kinds of critical velocity should reflect the existence of two different mechanisms of vortex formation.

The extrinsic critical velocities are presumably due to the growth of preexisting vorticity as suggested by various vortex mill models.[11] Their values cannot be made reproducible, as they depend on the configuration of the vortices pinned nearby the hole. In fact, the position of the pinned vortices may be changed either by thermally cycling the experimental apparatus or simply by reversing the flow direction.

The intrinsic dissipation was first detected by avoiding the motion of the preexisting superfluid vorticity by means of some porous medium placed in front of the hole.[3,4,12] The temperature dependence of the intrinsic critical velocity suggests that thermal vortex fluctuations play an important role in the vortex production. In fact, a model based on the thermally activated production of quantized vortex rings (the ILF model)[13] accounts for the qualitative temperature behavior of the critical velocity above 1 K.

In an attempt to obtain a superfluid ^{4}He analog of the radio-frequency (rf) SQUID which could be used as a gyroscope,[14,15] we have had the opportunity to make ac measurements of critical velocities in superfluid ^{4}He in the 1.2–2.11-K range. In our experiment we forced a

flow through a little orifice with an unusual method that, in the past, had given unclear results.[16] We used a hollow torus filled with HeII. The torus was interrupted by a septum with an orifice 5 μm in radius, and a hydrodynamic superflow was induced through the hole by torsionally oscillating the whole torus. The results of the measurements made are reported hereafter.

II. EQUILIBRIUM STATES OF THE SUPERFLUID IN A ROTATING TORUS

In this section we will calculate the velocity of the superflow in our torus and the equilibrium states of the superfluid as a function of the angular velocity Ω_t of the torus itself. We will follow the outline given in Ref. 14, adapting it to the "weak-link" case. The calculation is based on the fact that the superfluid velocity field $\mathbf{v}_s$ is related to the φ phase of the complex order parameter by the equation

$$\mathbf{v}_s=(k/2\pi)\nabla\varphi \ , \tag{1}$$

as in the classical flow of a perfect fluid with potential $(k/2\pi)\varphi$; here $k=h/m_4$ is the quantum of circulation. We will also use the existence of a critical velocity for the flow through the orifice and the quantization of the circulation in the inertial frame in its usual form:

$$\oint \mathbf{v}_s\cdot d\mathbf{l}=nk \tag{2a}$$

or the equivalent

$$\oint \nabla\varphi\cdot d\mathbf{l}=2\pi n \ , \tag{2b}$$

where n is an integer.

The following calculation is not influenced by the existence of some preexisting vorticity in the superfluid, provided that these vortex lines are not allowed to move around in the liquid. In fact, any such preexisting vorticity creates a persistent current in the vessel, thus producing the same effect as a steady rotation of the apparatus.[17] In practice, the preexisting vorticity may be prevented from moving by filling the helium vessel with powder or foam.

Consider now a torus of radius R and cross-sectional area σ, with $\sigma \ll \pi R^2$, filled with a mass $M_s \sim 2\pi R\sigma\rho_s$ of superfluid helium. The torus is interrupted by a septum with an orifice of radius r, with $\pi r^2 \ll \sigma$. According to the classical solution for the potential flow through an orifice in an unlimited plane,[18] the phase difference through the hole

$$\Delta\varphi=(2\pi/k)\int_\gamma \mathbf{v}_s\cdot d\mathbf{l} \ ,$$

where γ is a path passing through the hole, is

$$\Delta\varphi=(\pi I_m)/(k\rho_s r) \ , \tag{3}$$

where ρ_s is the density of the superfluid and I_m is the mass current through the hole. The difference is evaluated between two surfaces at distances δ from the hole with $\delta \gg r$. At this distance we assume the current density $J_s=\rho_s v_s$ to be uniform over the torus's section, so that v_s is, from now on, the average value of $\mathbf{v}_s$ in the torus away from the orifice. Moreover, $J_s=I_m/\sigma$, due to the continuity of the mass flow, and using Eq. (3) we may relate J_s to the phase difference through the orifice:

$$J_s=J_0\Delta\varphi \ , \tag{4}$$

where we define

$$J_0=\rho_s rk/(\pi\sigma) \ . \tag{5}$$

If we define a vector $\mathbf{J}_0$ with modulus J_0 and directed as the unit tangent vector, we may generalize Eq. (4) in a vectorial form:

$$\mathbf{J}_s=\mathbf{J}_0\Delta\varphi \ . \tag{6}$$

This relation holds only if $\mathbf{J}_s$ and $\Delta\varphi$ are measured in the reference frame at rest with the hole. If the torus is rotating about its axis with angular velocity Ω_t and tangential velocity $v_t=\Omega_t R$, we must subtract the tangential velocity and find a Galilei invariant relation between the same quantities measured in the inertial frame:

$$\mathbf{J}_s-\rho_s\mathbf{v}_t=\mathbf{J}_0\Delta\varphi^* \ , \tag{7}$$

where

$$\Delta\varphi^*=\Delta\varphi-(2\pi/k)\int_\gamma \mathbf{v}_t\cdot d\mathbf{l} \tag{8}$$

represents the phase shift through the orifice measured by an observer at rest.

If we now eliminate J_s using Eq. (1), we obtain the value of $\nabla\varphi$ in the torus, as measured in the inertial frame, as a function of $\Delta\varphi^*$:

$$\rho_s\nabla\varphi(k/2\pi)=\rho_s\mathbf{v}_t+\mathbf{J}_0\Delta\varphi^* \ . \tag{9}$$

The superfluid must satisfy the quantization of circulation:

$$\Delta\varphi+\int_\Gamma \nabla\varphi\cdot d\mathbf{l}=2\pi n \ , \tag{10}$$

where the line integral is computed along a suitable path Γ in the torus, so that $\gamma+\Gamma$ is a closed circle. Substituting from Eqs. (8) and (9) for $\Delta\varphi$ and $\nabla\varphi$ as a function of $\Delta\varphi^*$ and then solving for $\Delta\varphi^*$, we get

$$\begin{aligned}&\Delta\varphi^*=2\pi(n-2\pi R^2\Omega_t/k)/\alpha \ ,\\ &\alpha=1+(2\pi R-\delta)2r/\sigma \ .\end{aligned} \tag{11}$$

As in our experimental apparatus (see below) $rR/\sigma \ll 1$; then $\alpha=1$.

Substituting $\Delta\varphi^*$ in Eq. (7), it is now possible to calculate the current density in the torus J_s and the mean velocity $v_h=I_m/(\pi r^2\rho_s)$ of the flow through the hole with respect to the rotating torus:

$$J_s=\rho_s[R\Omega_t+2r(nk-2\pi R^2\Omega_t)/\sigma] \ , \tag{12a}$$

$$v_h=(v_s-v_t)\sigma/(\pi r^2)=2(nk-2\pi R^2\Omega_t)/\pi r \ . \tag{12b}$$

For each value of n, the states described by these equations are metastable provided that

$$-v_c<v_h<v_c \ , \tag{13}$$

where v_c is a critical velocity characterizing the orifice.

When $v_h = v_c$, the state becomes unstable, and vortices appear in the hole. During their evolution, the highly inhomogeneous zone of the vortex core interacts with the normal fluid at rest with the boundary, thus making possible the exchange of energy and of angular momentum with the torus. If the time variation of Ω_t is much longer than the evolution time of the vortex and if the vortices generated at v_c cannot be pinned to the boundary, then the vortex core crosses all the irreducible paths in the torus during its evolution and finally annihilates at the boundary.[19] As a consequence, the superfluid is left in a different circulation state.

Working out Eq. (13) with the calculated value for v_h, we see that the n^{th} circulation state is a metastable state of the system only for angular velocities Ω_t satisfying the relation

$$(n-\tfrac{1}{2}v_c r\pi/k) < \Omega_t(2\pi R^2/k) < (n+\tfrac{1}{2}v_c r\pi/k) \ . \quad (14)$$

Different states are allowed for a given value of Ω_t, states that differ in the value of n. The number of allowed states N depends on v_c as $N = v_c r\pi/k$. At the two limiting values in Eq. (14), the system undergoes a transition to another circulation state with a value of n for which Eq. (14) still holds.

The angular momentum of the superfluid of total mass M_s is approximately $L_s = M_s v_s R$:

$$L_s = M_s R[R\Omega_t + 2r(nk - 2\pi R^2\Omega_t)/\sigma] \ , \quad (15)$$

so that the angular-momentum difference between two arbitrary circulation states depends at constant Ω_t only on the difference $n_2 - n_1$:

$$L_s(n_2) - L_s(n_1) = (n_2 - n_1)2M_s Rrk/\sigma \ . \quad (16)$$

If Ω_t sweeps between different values, hysteresis may occur with a related energy dissipation. For instance, suppose that $n = n_1$ and that Ω_t is increased starting from say $\Omega_t = n_1 k/(2\pi R^2)$. At $\Omega_t = \Omega_{c1}$ with

$$\Omega_{c1} = (n_1 k + \tfrac{1}{2}v_c r\pi)/(2\pi R^2)$$

a transition may occur to a state with different n, say $n = n_2$. The superfluid angular momentum takes a jump

$$\Delta L_s = L_s(n_2) - L_s(n_1)$$

and an energy $\Delta L_s \Omega_{c1}$ is transferred from the torus to the superfluid. If Ω_t is now decreased, the inverse transition may occur at $\Omega_t = \Omega_{c2}$ with

$$\Omega_{c2} = (n_2 k - \tfrac{1}{2}v_c r\pi)/(2\pi R^2)$$

and the energy $\Delta L_s \Omega_{c2}$ will be transferred back to the torus. If Ω_t is brought back to $\Omega_t = n_1 k/(2\pi R^2)$, the total energy dissipation in such an arbitrary cyclic transition will be

$$W_a = \Delta L_s(\Omega_{c1} - \Omega_{c2}) \ .$$

By using Eq. (16), we may write

$$W_a = (n_2 - n_1)M_s rk[v_c r\pi - (n_2 - n_1)k]/(\sigma\pi R) \ . \quad (17)$$

From this equation we may calculate the energy W_0 dissipated in an elemental transition $n \to n+1 \to n$:

$$W_0 \sim M_s r^2 k v_c/(\sigma R) = 2I_c k \ , \quad (18)$$

where the approximation works for $v_c r \gg k$; the critical average mass current is defined as $I_c = \pi\rho_s r^2 v_c$. Given the actual dimensions of our torus, as described in the following section, the expected value of W_0, at a typical critical velocity of 1 m/sec, is about 10^{-15} J.

When

$$n_2 - n_1 \sim v_c r\pi/(2k) \ ,$$

the dissipated energy W_a reaches its maximum value W_m:

$$W_m \sim W_0 v_c r\pi/(4k) \quad (19)$$

that may be calculated to be about 10^{-13} J.

III. APPARATUS

In our apparatus the torus is the inertial member of a torsional pendulum. This way we can easily modulate Ω_t by driving the pendulum at its resonance angular frequency ω_0. In this configuration, depending on experimental conditions, the occurrence of dissipation can be seen either as a reduction of the effective quality factor of the oscillator, or as a sudden collapse in the oscillator amplitude.

The torus used in the experiment was made of three aluminum pieces glued together with epoxy resin (Fig. 1): a hollow cylinder closed at the bottom, a flat top flange, and a central bulk cylinder connecting the other two pieces. In the central cylinder, two 0.5-mm holes were drilled: the first one along the cylinder axis, from one end to the center, the second one along its diameter, from the center to the surface. The resulting right-angle-shaped channel formed the final part of the helium filling line. At the upper end of this channel, a phosphor bronze tube 0.4-mm outer diameter (o.d.) and 0.1-mm inside diameter (i.d.) and 20-mm long was glued. This tube served both as a continuation of the filling line and as the torsion member of the oscillator. The mean radius R of the resulting inner cavity of the torus was 7 mm, and the cross section σ measured 60 mm^2. The torus was filled with helium by condensing the gas through a capillary tube from a high-pressure cylinder placed outside the cryostat. To keep the liquid at its vapor pressure, one end of the filling line was led into a cold pot half-filled

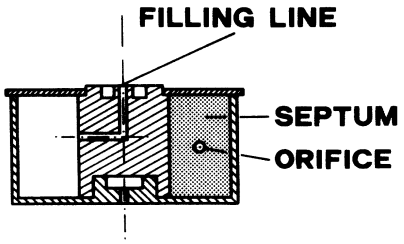

FIG. 1. Schematic drawing of the torus assembly with the filling line and the septum; the orifice is not to scale.

with liquid (Fig. 2). A second piece of capillary tube connected the pot with the torsion member and, through this, with the torus. This second piece of filling line was therefore always full of liquid during the measurements.

To stop the superfluid vorticity,[12] the filling line outlet into the torus was guarded by a porous filter (UM2 Diaflo microfiltration membrane with a 1000 molecular weight cutoff) glued with precured epoxy. On the opposite side of the torus from the filling line outlet, a copper septum was glued, which supported a free-standing 5-μm nickel foil with an orifice 5 μm in radius (Fig. 1). In order to stop the motion of the preexisting vortex lines, an open-cell foam filled the torus except for a 5-mm zone on both sides of the septum. This zone was left empty in order to allow a free evolution of the vorticity generated in the orifice.

In order to stabilize the direction of the oscillator axis and to shift the frequency of transverse motion away from the torsional resonance, a nylon filament 0.2 mm in diameter was glued to the bottom of the torus and tensioned by means of a BeCu spring. The moment of inertia of the empty torus was $I_t \sim 1.5\times10^{-7}$ kg m^2, the mass and moment of inertia of the helium inside the torus were about 0.23 g and 9×10^{-9} kg m^2, respectively.

A forcing torque was applied by means of an electrostatic transducer made of two opposite pairs of fixed electrodes acting on two grounded plates. The plates had areas $A=6\times8$ mm^2 and were glued to the torus, again on opposite sides (Fig. 3). The same constant high-voltage bias V_H relative to the ground was applied to all four fixed electrodes. An alternating potential difference was also applied to the electrode system by means of a transformer. This was done in such a way that a potential $V_H+\beta V_d\sin(\omega_0 t)$ relative to the ground was applied to one set of diagonally opposite fixed plates while the potential $V_H-\beta V_d\sin(\omega_0 t)$ was applied to the other set. To first order, only torsional modes were excited by this bias scheme. Here $\beta=0.41$ is the transformer ratio of the

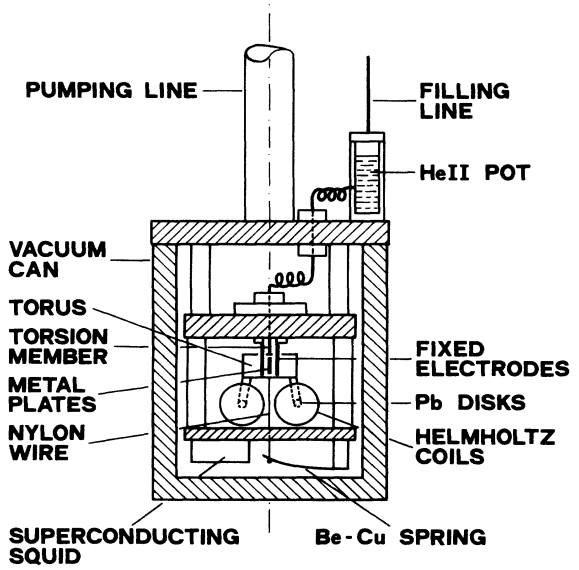

FIG. 2. Schematic drawing of the experimental apparatus.

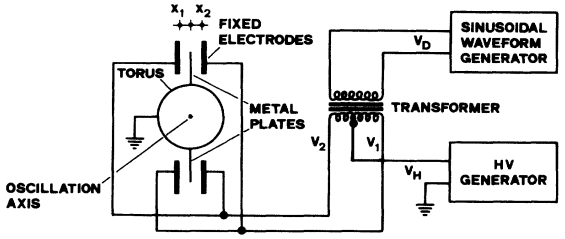

FIG. 3. Schematic drawing of the driver with the control electronics.

decoupling transformer at the excitation frequency and V_d is the peak amplitude at the generator output. The force acting on each plate depends on the two distances x_1, x_2 between the plate itself and the fixed electrodes facing it. In the simplest case, $x_1=x_2=x_0$, the peak torque acting on the torus was

$$T_A \sim 2bV_d\beta V_H\varepsilon_0 A/x_0^2 , \tag{20}$$

where $b\sim14$ mm is the average distance of a plate from the axis. At a dc bias voltage of 119 V and with $x_0=1.5$ mm, we estimated this torque to be

$$T_A/V_d=(1.6\pm0.8)\times10^{-9}\ \text{N m/V} . \tag{21}$$

The large uncertainty in this estimate is due to the difficulty both in evaluating the equilibrium values of x_1 and x_2 and in controlling the planarity of the whole system.

The angular displacement of the torus was measured by means of a detector made of two superconducting disks of radius $a_d=1.2$ mm. The disks were attached to the torus at $R=10$ mm from the axis (Fig. 4) and moved in a uniform magnetic field B_0 generated by two systems of 64-turn superconductive Helmholtz coils, 9 mm in radius. Due to the Meissner effect, each superconducting disk changes both the distribution of the magnetic field and (consequently) the flux Φ_e through a pair of superconducting coils located in front of it. Each sensing coil, of radius $a_c=2.5$ mm, was made of 10 turns of 0.075-mm Nb wire. The effective area of each coil $A(z)=\Phi_e/B_0$ is a function of the distance z between the disk and the coil itself.[20] For small displacements around the equilibrium position, $z=a_c$, and with $a_d=\frac{1}{2}a_c$, as in our configuration, one can estimate $\partial A(z)/\partial z\sim2.8$ mm.

To reject stray fields, the two coils facing each disk

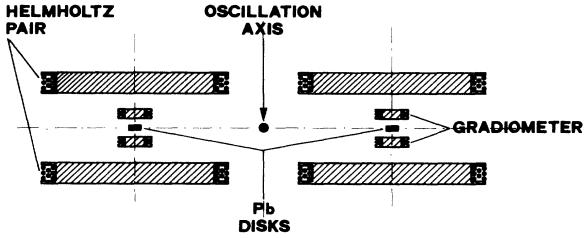

FIG. 4. Schematic drawing of the torsional position sensitive detector.

were connected in a series in a gradiometer configuration. The two gradiometers were then connected in a series so that the resulting transducer should be sensitive to torsional oscillations and should reject the signals coming from pendulum oscillations. The calculated total inductance of the four coils was about 4.5 μH. The four sensing coils were part of a flux transformer, coupled by means of a Nb coil to a homemade two-hole SQUID, read with commercial 19-MHz electronics.[21] The 1.4-mm-diam coupling coil was made of 100 turns of 0.075 mm Nb wire. The inductance of this coil was found to be 3.5 μH, and the mutual inductance with the SQUID was estimated to be ~ 10 nH. From the resulting transformer ratio value $t_f = 1.3\%$, we calculated the angular sensitivity of the transducer:

$$\partial \Phi_s / \partial \vartheta \sim 4 B_0 R t_f \partial A(z)/\partial z \ , \tag{22}$$

where Φ_s is the flux signal at the SQUID.

Because of a loose contact in the closed superconducting circuit made of the four Helmholtz coils, we could only use a current of 3.3 mA, which produced a field intensity $B_0 = 1.5 \times 10^{-4}$ T. Given this field figure and the above reported value for $\partial A/\partial z$, we estimated the angular sensitivity as

$$\partial \Phi_s / \partial \vartheta \sim (1.0 \pm 0.3) \times 10^3 \Phi_0 / \text{rad} \ , \tag{23}$$

where $\Phi_0 = 2.07 \times 10^{-15}$ Wb is the magnetic flux quantum. The large uncertainty in this estimate is mainly due to the uncertainty of the estimated equilibrium position of the superconducting disks. With a typical flux noise of $5 \times 10^{-4} \Phi_0 / \sqrt{\text{Hz}}$, we get an angular resolution of 5×10^{-7} rad$/\sqrt{\text{Hz}}$.

The whole system of the torsional oscillator, the forcing plates, and the position detector was enclosed in an evacuated oxygen-free high-conductivity copper can. The can was, in turn, enclosed in a superconducting lead shield.

In order to reduce the mechanical noise, the cryostat was put on a 120-kg foundation resting on four inflated motorcycle tubes. All vacuum lines were made with rubber tubing. Each line was anchored to a 50-kg suspended mass placed at a distance of at least 2 m from the connection to the cryostat. Temperatures were measured by means of a calibrated Ge resistor. The estimated measurement error was about ± 2 mK; the temperature stability over the measurement time was about ± 3 mK. The base temperature of the system was ~ 1.2 K.

The resonant frequency of the empty torus was 31.403 ± 0.002 Hz; the error figure also takes into account the variations from run to run. The Q factor, measured from the free-oscillation decay time τ according to the formula $Q = \tau \omega_0 / 2$, was about 5×10^4 at 4.2 K. The resonance was excited with a high-stability synthesized oscillator HP3325B, also used as the reference input for a lock-in amplifier that read the angular position signal at the SQUID output (Fig. 5). The amplitude and phase of this signal with respect to the forcing torque were A/D converted; they were then acquired by a desktop computer. The frequency of the synthesized oscillator was controlled by the computer and automatically adjusted in order to keep the value of the phase at 90°. This digital feedback control arrangement was used to track the long-term drifts of the torus resonance frequency.

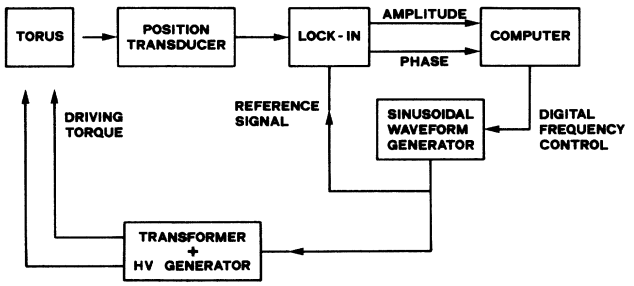

FIG. 5. Schematic drawing of the resonance stabilization electronics.

Once the torus was completely filled with liquid helium, its resonance frequency was 30.35 ± 0.05 Hz; as before, this error includes the variations from run to run. The reduction from the value found when the torus was empty was consistent with our estimate of the moment of inertia of the liquid. The quality factor with the torus full of helium was found to depend on the temperature; the lowest value $Q = 300$ was observed at 4.2 K with the torus filled with normal fluid, the maximum value, about $Q = 1200$, was found at 1.2 K.

IV. EXPERIMENTAL RESULTS

Typical experimental results regarding the oscillation peak amplitude ϑ_A as a function of the excitation peak torque T_A at different temperatures are reported in Fig. 6. At every given temperature, a set of values of ϑ_A were automatically recorded as the excitation voltage V_d was increased in steps ΔV_d. A time of $\sim 5\tau$ was allowed to elapse after each drive voltage step increase ΔV_d before the relative amplitude measurement was made. The

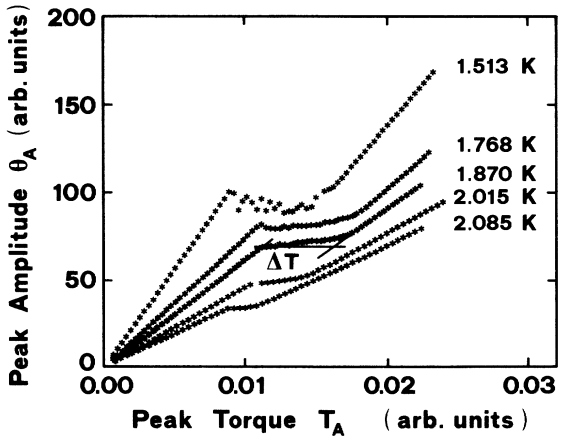

FIG. 6. Torus oscillation peak amplitude ϑ_A vs driving torque peak amplitude T_A at different temperatures. From the estimated calibration of the position detector and the torque transducer, the amplitude unit corresponds to 1 μrad with a 30% accuracy and the torque unit corresponds to 10^{-7} $N\,m$ with a 50% accuracy.

free-oscillation decay time τ was measured before each set of measurements was taken. Each measurement of ϑ_A was a 5-min average of the lock-in output; the lock-in time constant was 1 sec in all of the measurements reported in this section. The curves drawn in Fig. 6 were all obtained by increasing T_A; however, we never observed any difference in the measurements obtained by decreasing T_A.

In these plots we distinguish three separate regions: first, when the torus oscillates at low amplitude, in the region from now on called subcritical, ϑ_A is a linear function of the torque T_A, in agreement with the standard theory of the forced resonator: $\vartheta_A = T_A Q/(I_t \omega_0^2)$. In this subcritical region the inverse of the quality factor is roughly proportional to the normal fluid fraction plus a constant (Fig. 7). Second, at each temperature a plateau is clearly recognizable in the data. In this plateau region the torus no longer acts as a linear passive device, and the peak oscillation amplitude on the plateau is almost independent of the drive torque. The starting point of the plateau, from now on called the critical point, was observed to be reproducible, within the experimental errors, both in the torque and in the oscillation amplitude, and both within the same run and after cycling the system to 4.2 K. Third comes a supracritical region, where the oscillation amplitude again increases monotonically as a function of the drive.

With the chosen 5-min integration time, the reading error in the amplitude measurement is about 0.1% in the subcritical and supracritical regions. In the plateau region, the spreading of the experimental points is much larger, due to the occurrence of distinct events of the sudden reduction of the oscillation amplitude, of total duration ~ 30 sec, followed by a slower recovery process (Fig. 8). These events are hardly distinguishable at temperatures close to T_λ, but they become very evident at lower temperatures. Below 1.6 K, the averaging procedure within the plateau region is much more difficult because of the above-mentioned processes. From the signal oscillation amplitude reduction, it is possible to estimate the corresponding reduction of the torsional oscillation amplitude $(\vartheta_2 - \vartheta_1)$ and the typical energy lost by the oscillator

$$\Delta E_k = \tfrac{1}{2} I_t \omega_0^2 (\vartheta_2^2 - \vartheta_1^2) .$$

This amounts, for instance, to about 5×10^{-13} J in each of the events shown in Fig. 8(a). The oscillation amplitude just before each event and the amount of the subsequent amplitude reduction are not reproducible; on the contrary, they vary, at constant drive level, by as much as 1 order of magnitude.

The dissipation process involved in each of the events shown has surely come to an end before the next one occurs, as indicated in Fig. 8(a). In fact, the characteristic recovery time constant just before an event is the same as the free-oscillation decay-time constant in the subcritical region, which indicates the absence of any excess dissipation in the superfluid during the recovery process. As shown in Fig. 8(b), which refers to data still in the plateau region but at a higher value of V_d, the total recovery time decreases as the drive voltage increases. As a consequence, the dissipative events in the plateau region tend to become less distinguishable. In fact, a constant excess dissipation takes the place of the distinct dissipative events, and there is a smooth transition into the supracritical region, where the error in the amplitude measurements is again 0.1%. Now the oscillation amplitude increases again, which indicates that, in each oscillation cycle, the driving torque feeds back the energy lost by the oscillator. The slope in the supracritical region is significantly smaller than the slope below the critical

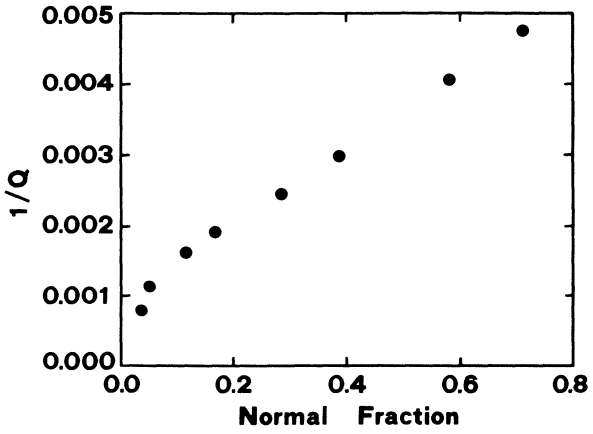

FIG. 7. Inverse of the quality factor Q of the torus as a function of the normal fraction of the liquid.

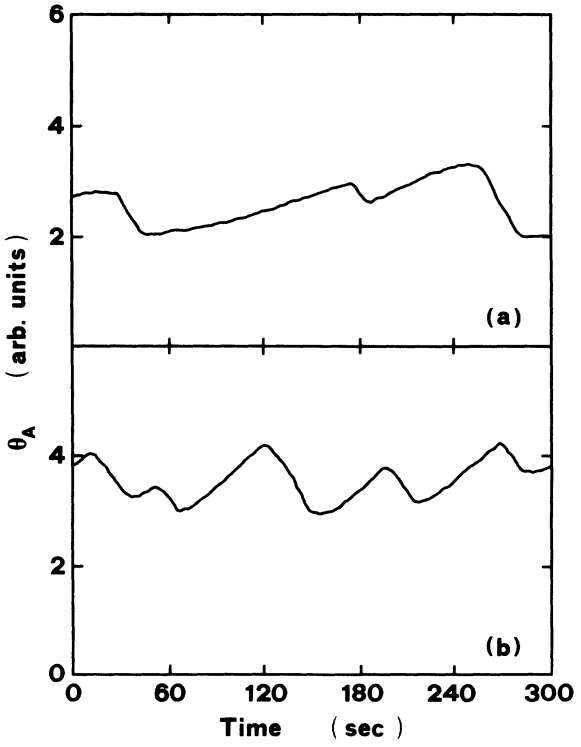

FIG. 8. Temporal dependence of the oscillation amplitude in the plateau region at 1.5 K with two different peak drive voltage values: (a) $V_d = 0.65$ V and (b) $V_d = 0.9$ V.

point, which confirms that the superfluid dissipates a certain amount of energy during each oscillation cycle.

In separate experiments we looked at the decay of free oscillations starting from a given oscillation amplitude. In close agreement with these results, the decay of free oscillations starting from a supracritical value showed a sudden increase in the decay time (proportional to the quality factor) when the amplitude crossed the level corresponding to the plateau (Fig. 9). We observed that, at each temperature, these free decay times $\tau_<$ and $\tau_>$, measured in the supracritical and subcritical region, respectively, are about the same as the typical decay time and recovery time in the dissipative events on Fig. 8.

In Fig. 10 we show the critical amplitude values ϑ_c as a function of temperature. The units reported on the vertical scale can be read as μrad within a 30% accuracy. Corresponding values of the flow velocity in the orifice can be calculated from Eq. (12b) using $\Omega_t=\omega_0\vartheta_c$, supposing $n=0$:

$$v_c/\vartheta_c=4\omega_0R^2/r=(7\pm3)\times10^3 \text{ m/(sec rad)} . \quad (24)$$

Absolute calibration is now within 40% because of the uncertainty in the calibration of the values of ϑ_c and in the effective geometrical dimensions of the torus.

For a better understanding of the dissipation mechanism, we calculated the excess dissipation ΔW per cycle in the supracritical region. We used the obvious consideration that, to maintain a steady sinusoidal oscillation, the forcing system must compensate the energy dissipated by the friction in the oscillator. Just below the critical point, the driving torque supplies the work $W_1=\pi T_c\vartheta_c$ per cycle; at the end of the plateau it supplies the work $W_2=\pi(T_c+\Delta T)\vartheta_c$, where T_c is the torque at the critical point and ΔT is the width of the plateau along the torque axis. Then,

$$\Delta W=W_2-W_1=\pi\Delta T\vartheta_c .$$

We found the end point of the plateau by extrapolating to

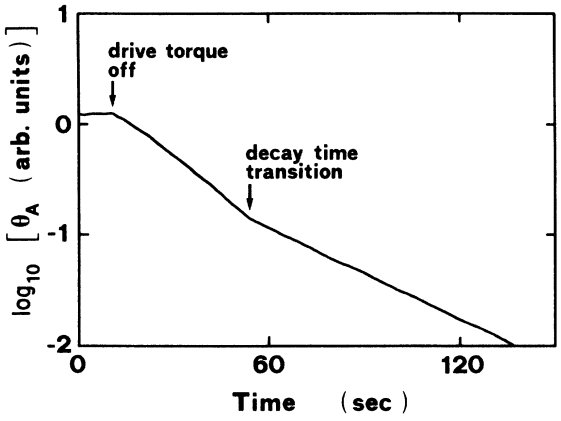

FIG. 9. Temporal dependence of the logarithm of the oscillation amplitude ϑ_A in the free decay from a supracritical point. The first arrow indicates the time at which the driving torque was stopped, the second arrow indicates the abrupt increase in the decay time. From these decay times we calculate the supracritical and subcritical Q values.

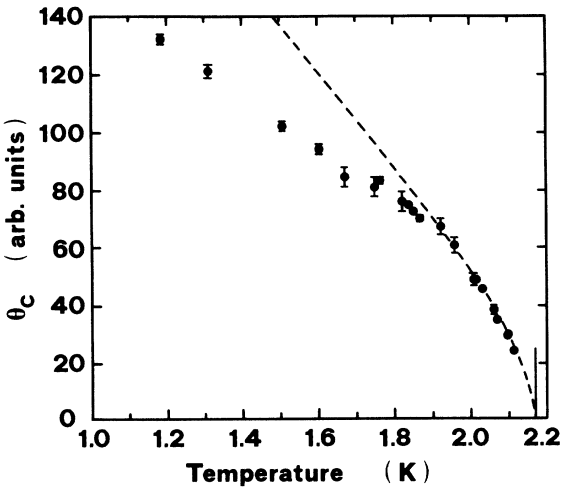

FIG. 10. Critical peak amplitude ϑ_c vs temperature. The vertical segment crossing the temperature axis identifies T_λ. The amplitude unit corresponds to 1 μrad with a 30% accuracy. Each experiment point represents a value of the critical velocity of the superfluid flow through the orifice; the conversion factor is $(7\pm3)\times10^{-3}$ m/(sec rad). Correspondingly, at full scale the velocity reading would be 1.0±0.4 m/sec. The dashed line is the function $\rho_s(T)T_\lambda/(\rho T)$ with arbitrary normalization.

ϑ_c a linear fit of the supracritical experimental points, as shown, for example, in the 1.870-K curve of Fig. 6. This way we did not take into account the details of the transition from the subcritical to the supracritical region. We think the related systematic error to be smaller than our calibration error in the torque and amplitude measurements. We cross checked these data by an independent method based on the quality factor reduction in the supracritical region. In fact, by using the definition $Q=2\pi W/w'$, where $W=\frac{1}{2}I_t\vartheta_A^2\omega_0^2$ is the energy stored in the resonant oscillation and w' is the energy dissipated in one oscillation cycle, we could calculate the excess dissipation ΔW at ϑ_c from the difference of the free-oscillation decay times in the subcritical and supracritical regions, $\tau_>$ and $\tau_<$ respectively,

$$\Delta W=2\pi I_t\vartheta_c^2\omega_0(1/\tau_<-1/\tau_>) . \quad (25)$$

Values of the dissipated energy per cycle calculated by both methods are shown in Fig. 11 as a function of the temperature. The agreement between the results obtained by the two methods is surprisingly good, despite the calibration error. This is due to the fact that the ratio of the results obtained by the two methods under the same conditions depends only on the ratio $\vartheta_c/\Delta T$. Absolute calibration of the ratio ϑ_A/T_A has been independently checked by considering that, in the linear regime, $\vartheta_A/T_A=Q/(I_t\omega_0^2)$. Using nominal calibrations for ϑ_A and T_A, we invariably found that this equation holds within the 10% accuracy within which I_t can be estimated. Although the nominal calibrations of angle and torque are uncertain by a larger amount than this, their uncertainties involve a common multiplicative factor.

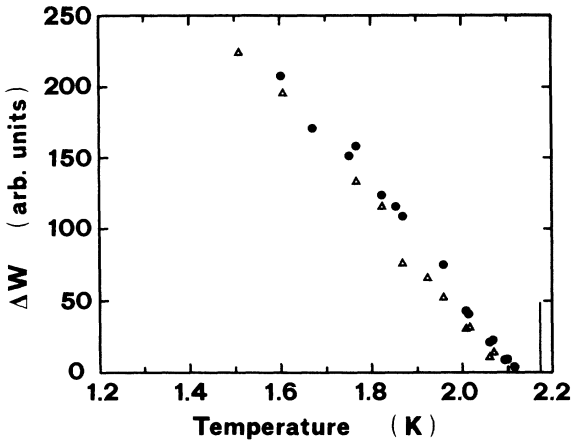

FIG. 11. Dissipated energy ΔW per cycle vs temperature. Triangles are calculated from the quality factor variation; circles are calculated from the plateau amplitude. The vertical segment crossing the temperature axis identifies T_λ. The energy unit corresponds to 10^{-15} J with an estimated calibration error of 50%.

V. DISCUSSION

The critical velocities [see Eq. (24)] corresponding to the data reported in Fig. 10 have the typical values and temperature behavior of the intrinsic critical velocities with a micrometric orifice. The data obtained for $T < 1.9$ K show a linear dependence on the temperature and extrapolate to zero at 2.65 ± 0.05 K, in reasonable agreement with the results obtained with the Helmholtz resonator technique, that extrapolate to zero between 2.41 and 2.55 K.[8,9] Data in this region also agree with those obtained by Hess in dc flow experiments, which are quite linear between 1.3 and 1.8 K and extrapolate to zero at $T \sim 2.56$ K.[3]

The high-temperature data, $1.9 < T < 2.115$ K, tend to zero at T_λ. As shown in Fig. 10, the data in this temperature range are well fitted by the function $A\rho_s(T)T_\lambda/(\rho T)$, where A is a fitting factor. This is in agreement both with what is found in gravitationally induced dc flows and with what is estimated by the ILF theory.[3,4] It must be noticed, however, that our data are not fitted by this theory if the whole temperature range is considered.

The existence of a critical velocity for the flow through the orifice accounts for the time behavior of the oscillation amplitude in the plateau region (Fig. 8). At the critical point, the rotationally induced superflow in the orifice reaches the critical velocity for vortex generation. The vortices give rise to an energy dissipation in the liquid and change the angular momentum of the superfluid, with a consequent reduction in the oscillation amplitude. The dissipation ends when the flow through the orifice has become subcritical during the whole oscillation period and all of the vortices involved have completed their evolution. Possibly related phenomena are reported in Refs. 6 and 7, where amplitude collapses in the oscillation amplitude of a Helmholtz resonator were observed. These collapse events occurred in less than one oscillation cycle, while, on the contrary, our reduction of the oscillation amplitude takes about 1000 oscillation cycles. We have no definite explanation for this large difference.

If all the vortices produced in the orifice were annihilated and the preexisting vortex line configuration remained unchanged, the calculations for the energy dissipated reported in Sec. II, should apply. In the absence of these conditions, however, we cannot quantitatively compare our data regarding the dissipated energy (Fig. 11) with any of the equations derived from Eq. (17). In fact, as stated before, our dissipative events involve many oscillation cycles, while Eq. (17) was obtained by supposing Ω_t to be almost constant during each circulation transition. We may only observe that the data for the excess energy loss per cycle ΔW are to the same order of magnitude as the maximum energy that can be dissipated in multiple transition events calculated by substituting the measured values of v_c in Eq. (19). The corresponding values of $n_2 - n_1 \sim v_c r\pi/(2k)$ range from 10 to 70.

Notice that, though ϑ_c, which we remind the reader is a 5-min average of the oscillation amplitude, is fairly reproducible, the value of the oscillation amplitude at which each dissipative event occurs is randomly distributed. This can be easily understood, as, at the end of each dissipative event, the oscillation amplitude is so much reduced that a number of "stable" circulation states are available. Thus, it is likely that the final circulation state is randomly chosen among these. As a consequence, the value of the oscillation amplitude just before the next dissipative event, that depends on the value of the circulation quantum [see Eq. (14)], is also a random variable.

The good reproducibility of the data recorded in the subcritical region is a consequence of the existence of at least one value of the circulation quantum n for which the stability condition in Eq. (14) holds for all the values taken by Ω_t during one oscillation period. In fact, the number of the states that satisfy this condition that we call, in short, stable states, is

$$N_A = 2\pi(\tfrac{1}{2}rv_c - 2R^2\Omega_A)/k \ ,$$

where $\Omega_A = \omega_0\vartheta_A$ is the amplitude of the angular velocity oscillation. N_A vanishes only for

$$\Omega_A \geq \omega_0\vartheta_c = rv_c/(4R^2) \ .$$

If this is not the case, and if the system, at the beginning of the run, is occasionally not in one of these stable states, it will soon reach it after a few transitions. In fact, energy dissipations occurring during these occasional transitions have been sometimes observed in the subcritical region at the beginning of the 5τ waiting time after each drive change. On the contrary, at amplitudes above ϑ_c, "stable" states are no longer available and the system is forced to undergo the transitions with the characteristic behavior of the critical regime.

It must be noticed that both the fair reproducibility of the critical amplitude ϑ_c and the unpredictability of the value of the oscillation amplitude just before a single dissipative event can also be explained if the vortices produced become steadily pinned somewhere in the torus.

In fact, any distribution of vortices pinned on surface imperfections will induce a steady unknown superflow through the orifice that adds to the rotationally induced one.[17] This unpredictable superflow would also contribute to randomize the amplitude at which the dissipative events take place. Moreover, in accord with the previous discussion, in the subcritical region, after a few transitions the system would be allowed to reach a "stable" configuration of vortices. This would occur when the total superflow contributed both by the system of pinned vortices and by the torsional oscillation stays lower than the critical superflow during the whole oscillation period.

VI. CONCLUDING REMARKS

We observed a rotationally induced dissipation in superfluid ^{4}He. Considering the reproducibility of the critical amplitude and the temperature behavior, we attributed this dissipation to the formation of "intrinsic" vortices in the orifice at the critical flow rate. Our work extends, up to 2.115 K, the ac flow measurements of critical velocities performed with Helmholtz resonators.

The reproducibility of the critical velocity data, their temperature dependence, and the essential agreement between data obtained in different experiments suggest that a thermal nucleation mechanism is involved in the intrinsic formation of vortices, as the critical processes involving the depinning of preexisting vorticity can hardly account for the homogeneity of data obtained with different orifices. However, the ILF nucleation model cannot account for the data in the whole 5 mK to 2.1 K range.

In conclusion, let us make, a few remarks on the implications of our observations for the realization of the analog of the SQUID mentioned in the Introduction. In order to get proper SQUID behavior, jumps are needed in the circulation quantum of $|\Delta n|=1$ at the critical velocity. If this limit were reached, then the perfect analog of the staircase pattern of the superconducting rf SQUID should be evidenced in the ϑ_A versus T_A plot. Any quasistatic superimposed angular velocity would then periodically modulate this pattern, again in analogy with the SQUID.[14,15] Though this second phenomenon has never been observed, a staircase pattern has been reported in one of the experiments made with Helmholtz resonators.[22] The energy dissipation measured in our experiment is consistent with jumps of the circulation quantum n with $|\Delta n|>10$, and this is probably why it was not possible for us to observe the expected SQUID behavior with our experimental apparatus. In our opinion, the number Δn of circulation quanta the system actually jumps in a single transition depends on various more or less relevant parameters.

First, the number $N=v_c r\pi/k$, which represents the number of stable circulation states allowed at any specific angular velocity, should set an upper limit for $|\Delta n|$. N is just twice the so-called critical phase value in units of 2π,[4] $\Delta S_c^*/(2\pi)=N/2$. Having $N\sim 1$ may not be greatly important, since Avenel and Varoquaux observed single quantum transitions with $N\sim 26$.[22] However, if N proved to be a relevant parameter, it could be reduced either by diminishing r to less than 1 μm, as in Refs. 5 and 7, or by operating at temperatures close to T_λ, where v_c is smaller. This last possibility is permitted by the fact that the quality factor of our oscillator with the 5-μm radius orifice appears to severly degrade only for temperatures above 2.1 K.

Second, to inhibit random multiple transitions, the evolution time of a single vortex should be shorter at least than the flow oscillation period. In fact, the staircase pattern was obtained with a low-frequency ($\nu_0\sim 2$ Hz) Helmholtz resonator,[22] while single transitions were not reported in a similar experiment operating at ~ 1 KHz.[5] These considerations seem to indicate that the frequency of operation is another relevant parameter that needs to be changed in order to reach the single-transition limit. However, in order to make a superfluid SQUID act as a practical gyroscope, the frequency cannot be lowered at will. The problem may be solved again by working at temperatures close to T_λ, where a high fraction of normal fluid is present and the vortex evolution is faster. It seems that both the conditions discussed above can be met in the kind of experimental method we have presented in this paper.

ACKNOWLEDGMENTS

The micrometric orifice used in the experiment was prepared by Dr. C. Camerlingo and Dr. G. Jung. We are also indebted to R. Dallapiccola, F. Gottardi, and T. Ropelato for their technical help.

*On leave from Dipartmento di Fisica, Università degli Studi di Trento, I-38050 Povo, Trento, Italy.

[1]V. P. Peshkov, in *Progress in Low Temperature Physics,* edited by C. J. Gorter (North-Holland, Amsterdam, 1964), Vol. IV, p. 1.

[2]J. P. Hulin, C. Laroche, A. Libchaber, and B. Perrin, Phys. Rev. A **5**, 1830 (1972).

[3]G. B. Hess, Phys. Rev. Lett. **27**, 977 (1971).

[4]J. P. Hulin, D. D'Humieres, B. Perrin, and A. Libchaber, Phys. Rev. A **9**, 885 (1974).

[5]B. P. Beecken and W. Zimmermann, Jr., Phys. Rev. B **35**, 74 (1987).

[6]G. B. Hess, Phys. Rev. B **15**, 5204 (1977).

[7]O. Avenel and E. Varoquaux, Phys. Rev. Lett. **55**, 2074 (1985).

[8]B. P. Beecken and W. Zimmermann, Jr., Phys. Rev. B **35**, 1630 (1987).

[9]E. Varoquaux, M. W. Meisel, and O. Avenel, Phys. Rev. Lett. **57**, 2291 (1986).

[10]E. R. Huggins, Phys. Rev. A **1**, 332 (1970).

[11]W. I. Glaberson and R. J. Donnelly, Phys. Rev. **141**, 141 (1966); K. W. Schwarz, Phys. Rev. Lett. **64**, 1130 (1990).

[12]D. D'Humières and A. Libchaber, J. Phys. (Paris) Colloq. **39**, C6-156 (1978); L. R. Foreman and H. A. Snyder J. Low. Temp. Phys. **33**, 243 (1978).

[13]J. S. Langer and M. E. Fisher, Phys. Rev. Lett. **19**, 560 (1967); S. V. Iordanskii, Zh. Eksp. Teor. Fiz. **48**, 708 (1965) [Sov. Phys.—JETP **21**, 467 (1965)].

[14]M. Cerdonio and S. Vitale, Phys. Rev. B **29**, 481 (1984).

[15]M. Bonaldi, Ph.D. thesis, Università di Trento, 1990.
[16]R. W. Guernsey, Jr., in Proceedings of the 12th Conference on Low Temperature Physics, edited by E. Kanda (Keigaku, Tokyo, 1971); D. D. Gregory and J. M. Goodkind (private communication).
[17]E. B. Sonin, Usp. Fiz. Nauk **137**, 267 (1982) [Sov. Phys.—Usp. **25**, 409 (1982)].
[18]P. M. Morse and H. Feshback, *Methods of Theoretical Physics* (McGraw-Hill, New York, 1953), p. 1294.
[19]G. E. Watson, J. Low Temp. Phys. **31**, 297 (1977).
[20]J. A. Owerweg and M. J. Walter-Peters, Cryogenics **18**, 529 (1978).
[21]S. H. E. Model 330.
[22]O. Avenel and E. Varoquaux, Phys. Rev. Lett. **60**, 416 (1988).

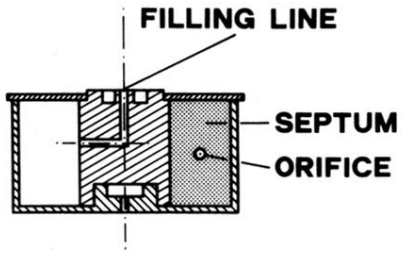

FIG. 1. Schematic drawing of the torus assembly with the filling line and the septum; the orifice is not to scale.